Fabrication of Periodic Sub-100nm Patterns in SiO_2 Template by Electron-beam Lithography

A. Chen[1], S. J. Chua[1, 2] and P. Chen[2]

[1]Singapore-MIT Alliance
E4-04-10, 4 Engineering Drive 3, Singapore 117576, ao.chen@nus.edu.sg
[2]Institute for Materials Research and Engineering
3 Research Link, Singapore 117602

ABSTRACT

We report on the fabrication process of SiO_2 templates with periodic sub-100nm air hole patterns using electron beam (e-beam) lithography and reactive ion etching (RIE). Two-dimensional square and hexagonal air hole arrays with sub-100nm dimensions were defined in 350-nm PMMA resist using a single-pixel exposure scheme by e-beam writing. The patterns in PMMA were then transferred into a 100-nm SiO_2 layer coated on GaAs or GaN/sapphire substrate by RIE. High-quality periodic air hole patterns in SiO_2 were achieved with the size ranging from 100nm to 52nm for the pitch of 200nm. Good pattern uniformity was also demonstrated and the deviation of air hole diameters was less than 4% in a pattern region of 100μm by 100μm. The SiO_2 template fabricated is very promising for the growth of periodic III-V semiconductor nanodots.

Keywords: nanodot; electron-beam lithography

1 INTRODUCTION

In recent years, ordered semiconductor nanostructures have attracted a lot of interest as they can greatly improve the performance of devices due to stronger quantum confinement effect. One extensively studied method to grow ordered nanostructures is to use nanoporous templates to control the nucleation sites. Locally ordered nanodots have been fabricated using nanochannel alumina prepared from self-organized anodic oxidation of aluminum [1-6]. However, the fabrication of templates with periodic nanoscale patterns of uniform size still remains challenging.

Here we report on an integrated fabrication process of SiO_2 templates with periodic sub-100nm air hole patterns using electron beam (e-beam) lithography and plasma dry etching. The whole process was developed on a 100-nm SiO_2 layer coated on GaAs and GaN/sapphire substrates, and is thereby applicable for a wide range of III-V semiconductor materials such as III-arsenide and III-nitride. The use of e-beam lithography enabled the generation of high-quality sub-100nm patterns, and precise pattern transfer into SiO_2 layer was realized by a well-controlled reactive ion etching (RIE) process. Details of the experiments and results of e-beam lithography and SiO_2 RIE will be presented in Section 2, and conclusions will be drawn in Section 3.

2 EXPERIMENTAL RESULTS

First a 100-nm thick SiO_2 layer was coated on the GaAs or GaN/sapphire substrate by Plasma Enhanced Chemical Vapor Deposition. Periodic sub-100nm patterns were then defined in the resist of PMMA 950K spin-coated on the SiO_2 layer by e-beam writing. After development and a short O_2 plasma descum process the patterns were transferred into the SiO_2 layer by RIE. The PMMA residue was finally removed by acetone and O_2 plasma clean.

2.1 E-beam Lithography

The e-beam writing was performed in the FEI Sirion 200 field emission scanning electron microscope (SEM) equipped with JC Nabity Nanometer Pattern Generation System. The writings were performed at the energy of 30keV, with a beam current of 20pA. The PMMA thickness was kept to be around 350nm, which was sufficient to be a durable etching mask for pattern transfer and at the same time thin enough for high-resolution e-beam writing.

The writing schemes to generate 2-D square and hexagonal dot arrays are illustrated in Figure 1. Square dot arrays were obtained by single-spot exposure of one rectangle, with the column and row spacing set by the exposure pixel spacing Δx and Δy respectively. Hexagonal dot arrays were produced by exposing the pixels of two overlapping rectangles with a proper displacement. As is shown in Figure 1(b), rectangle ABCD was first exposed with pixel spacing $\Delta y = \sqrt{3}\Delta x$, followed by the exposure of rectangle A'B'C'D' shifted by $(1/2\Delta x, \sqrt{3}/2\Delta x)$. As the error of beam movement between the two exposures increases with the field size, a small moving distance is favorable. To illustrate this idea the writing of a 200-nm pitch hexagonal dot array up to 100μm by 100μm was carried out in two different sequences: (a) the writing of the first rectangle ABCD ended at D and the second rectangle A'B'C'D' started from A'; (b) the first writing ended at C followed by the second one starting at C'. The corresponding beam movement involved is (0.1μm, -

99.8268μm) for (a) and (0.1μm, 0.1732μm) for (b). The results are given in Figure 2, where evident row displacement error was observed for (a), whereas well-aligned hexagonal dot array of 100μm by 100μm was achieved for (b).

Figure 3 shows the SEM images of square and hexagonal dot arrays produced in PMMA after e-beam exposure and development. Circular air holes were obtained from single-spot exposure due to the Gaussian beam profile. Proximity effect has put a limit on the spacing of dense patterns [7], and the minimum pitch achieved is 150nm for both square and hexagonal arrays. The hole size was simply determined by the dose for a given pitch, and a plot of the hole diameter as a function of the point dose is given in Figure 4. It was noticed that for certain dose range just above the threshold required for development patterns were formed in PMMA but not developed throughout the whole resist thickness of 350nm. Such patterns would fail to transfer during the following etching process, and the corresponding points are marked as hollow symbols in Figure 4.

In addition to the high-quality patterns, good size uniformity was also obtained. Statistical analysis of the hole diameters based on the SEM images randomly taken have shown a standard deviation of less than 4% for a pattern region of 100 μm by 100μm.

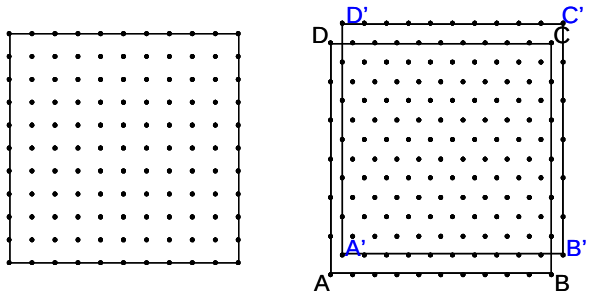

(a) (b)

Figure 1: Schematic diagrams of the e-beam writing schemes for (a) square dot array; (b) hexagonal dot array. The rectangles show the exposure area, while the solid dots represent the exposure pixels.

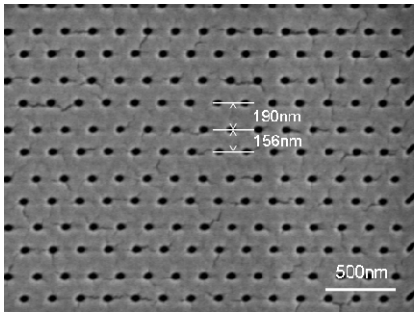

(a)

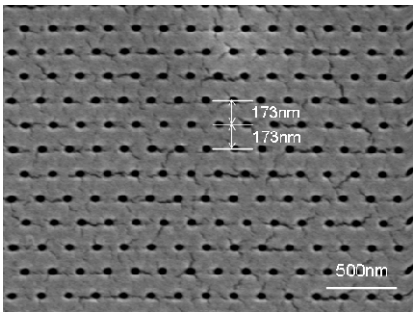

(b)

Figure 2: SEM images of hexagonal air hole arrays with 200nm pitch in PMMA after e-beam lithography. The writing order for the two rectangles ABCD and A'B'C'D' indicated in Figure 1(b) is (a) A, B, C, D, A', B', C', D'; (b) A, B, D, C, C', D', B', A'. The writing of each rectangle goes in the anti-clockwise direction and the stopping point is determined by the parity of the number of rows.

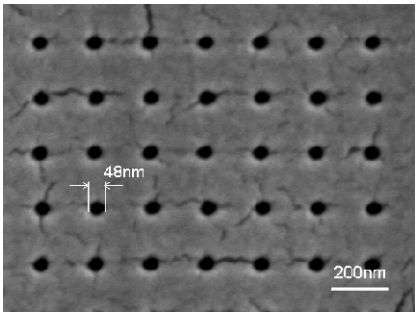

(a)

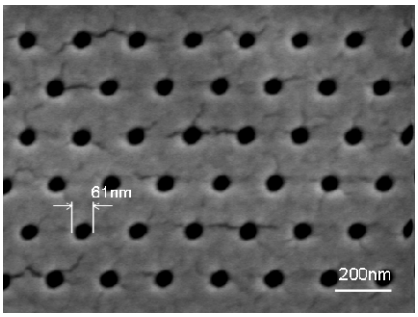

(b)

Figure 3: SEM images of periodic air hole patterns in PMMA after e-beam exposure and development. The air holes were organized into (a) square array with the pitch of 200nm; (b) hexagonal array with the pitch of 200nm.

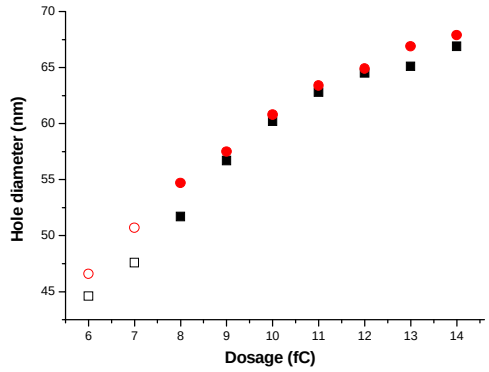

Figure 4: Plot of the air hole diameter as a function of the point dose used in e-beam writing for a square array with 200nm pitch (square symbols) and a hexagonal array with 200nm pitch (circular symbols). The solid symbols on the graph represent the patterns that could be transferred after SiO_2 etching, while hollow symbols represent those that failed to transfer.

2.2 SiO_2 Reactive Ion Etching

The patterns in PMMA were transferred into the SiO_2 layer by fluorine based RIE using Plasmalab80Plus from Oxford Instruments. The etching was carried out in a CHF_3 and Ar atmosphere, with the flow rate of 25sccm for each gas. The plasma was generated at the RF power of 150W, resulting in around 395V self-bias voltage at the pressure of 30mTorr. The CHF_3 gas offers high etch rate, vertical sidewalls and good selectivity over PMMA mask. As the exact etch rate is hard to measure due to the small pattern size, the minimum etch time required for a complete pattern transfer through the 100-nm SiO_2 layer was investigated. After RIE and removal of PMMA residue, the samples were dipped in a diluted H_3PO_4:H_2O_2 solution for a short time, which is a wet etchant for GaAs. The samples were then inspected by SEM after removing the SiO_2 layer by buffered HF solution, and small pits would form if the SiO_2 layer was etched through and GaAs surface was exposed. Such optimized etch time would allow durable pattern transfer and minimize the plasma-induced damage to the substrate as well. The etch rate of SiO_2 on GaAs substrate evaluated this way is also applicable for that on GaN/sapphire substrate, and periodic InGaN nanodots have been successfully grown on the GaN/sapphire substrate using the SiO_2 template fabricated [8].

Fig. 5 shows the SEM images of square and hexagonal air hole arrays in the SiO_2 template fabricated on GaAs substrate. Precise pattern transfer from PMMA to SiO_2 was achieved with a slight size increase less than 5%, and the minimum hole size achieved is 52nm for the pitch of 200nm in the SiO_2 template. Furthermore, good size uniformity was also transferred into SiO_2, with the standard deviation less than 4% in a dot array of 100 µm by 100µm.

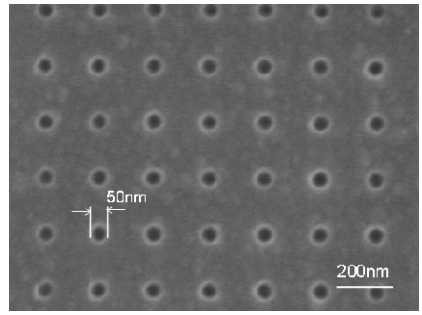

(a)

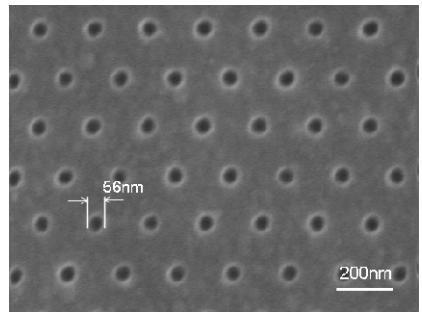

(b)

Figure 5: SEM images of periodic air hole patterns in SiO_2 fabricated on GaAs substrate. The air holes were organized into (a) square array with the pitch of 200nm; (b) hexagonal array with the pitch of 200nm.

3 CONCLUSION

We have demonstrated the fabrication of SiO_2 templates with periodic sub-100nm patterns on GaAs and GaN/sapphire substrates. Periodic air hole patterns organized into square and hexagonal arrays were produced with the diameter ranging from 100nm to 52nm for 200-nm pitch. Good pattern size uniformity was also obtained, with the size deviation less than 4% in a 100µm by 100µm filed. This method can be used for the growth of periodic nanostructures over a wide range of III-V semiconductor materials, and is also applicable for the fabrication of other periodic nanostructures such as nano-wires and nano-rings.

REFERENCES

[1] Q. Guo, X. Mei, H. Ogawa and H. Ruda, Jpn. J. Appl. Phys. 41, 7297, 2002.
[2] X. Mei, D. Kim, H. E. Ruda and Q. X. Guo, Appl. Phys. Lett. 81, 2002, 361.
[3] X. Mei, M. Blumin, M. Sun, D. Kim, Z. H. Wu, H. E. Ruda and Q. X. Guo, Appl. Phys. Lett. 82, 967, 2003.
[4] Q, Guo, X, Mei, H, Ruda, T. Tanaka, M. Nishio and H. Ogawa, Jpn. J. Appl. Phys. 42, 508, 2003.
[5] P. Chen, S. J. Chua, Y. D. Wang, M. D. Sander and C. G. Fonstad, Appl. Phys. Lett. 87, 143111, 2005.

[6] W. L. Xu, M. J. Zheng, G. Q. Ding and W. Z. Shen, Chem. Phys. Lett. 411, 37, 2005.
[7] M. A. McCord and M. J. Rooks, "Handbook of microlithography, micromachining, and microfabrication: volume 1", SPIE Optical Engineering Press, 139-248, 1997.
[8] A. Chen, S. J. Chua, P. Chen and X. Y. Chen, unpublished.